Available online at www.sciencedirect.com
ScienceDirect
Journal of Bionic Engineering 5 (2008) 95−101

Parametric Research of Experiments on a *Carangiform* Robotic Fish

Qin Yan, Zhen Han, Shi-wu Zhang, Jie Yang

Department of Precision Machinery and Precision Instrumentation, University of Science and Technology of China, Hefei 230026, *P. R. China*

Abstract

In this paper, a *carangiform* robotic fish with 4-DoF (degree of freedom) tail has been developed. The robotic fish has capability of swimming under two modes that are radio control and autonomous swimming. Experiments were conducted to investigate the influences of characteristic parameters including the frequency, the amplitude, the wave length, the phase difference and the coefficient on forward velocity. The experimental results shown that the swimming performance of the robotic fish is affected mostly by the characteristic parameters observed.

Keywords: biomimetic, robotic fish, experimental parameter matrix, undulation equation, body length velocity

1 Introduction

Fish show excellent swimming performance in nature, so more and more researchers have focused on mimicking fish locomotion for developing underwater vehicle with high speed, high maneuverability and high efficiency. With the integration of biological theory and engineering practice, Autonomous Underwater Vehicles (AUV) have been developed and applied to civil or military areas.

Fish locomotion can be classified into two categories on the basis of the propulsive mechanism used: Body and/or Caudal Fin (BCF) mode in which fish swim with their body and/or caudal fin and Median and/or Paired Fin (MPF) mode in which fish propel with their media and/or paired fin[1]. BCF mode displays the outstanding performance of high speed and high efficiency, while MPF mode is capable of maintaining good stability. Both types of the propulsion modes have been studied in detail. The first robotic fish, Robotuna, developed by MIT[2] in 1994, swims at a velocity up to 2 $m \cdot s^{-1}$ by swinging posterior body and lunate tail. Mason and Burdick[3,4] developed a *carangiform* prototype and underwent the experiment to testify the supposition of thrust generated from swinging fin. To improve the maneuvering control, Kato laboratory carried out the research on the pectoral fin control[5]. Liu *et al*.[6–8] developed autonomously fish-like robot on the basis of the inspiration from biological system. Low *et al*.[9–11] showed interest in undulation mechanism propelling by the undulating fins.

In this paper, a *carangiform* robotic fish prototype was presented to investigate the influences of the characteristic parameters on the forward velocity. This study described the mechanical configuration and the electronic system of the robotic fish, and investigated the influences of several important parameters on the velocity.

2 Materials

2.1 Mechanical design of the robotic fish

Fig. 1 shows the mechanical structure of the robotic fish developed in the present work. The robotic fish consists of two parts mainly: head module and body section. The head module that is made of fibre glass has enough rigidity to resist the pressure. It also has enough space to hold the control system, battery and the counterweight. There are three holes on the head module for installing the infrared sensors, on where is the front, left and right. The body section includes joints, strut members and caudal fin. The four scale-down joints are

Corresponding author: Qin Yan
E-mail: yanqin@mail.ustc.edu.cn

connected in series for generating the wave motion. The strut members are used to support a flexible plastic tube which prevents the servomotor from water. The caudal fin is made of a thin deformable plastic plate.

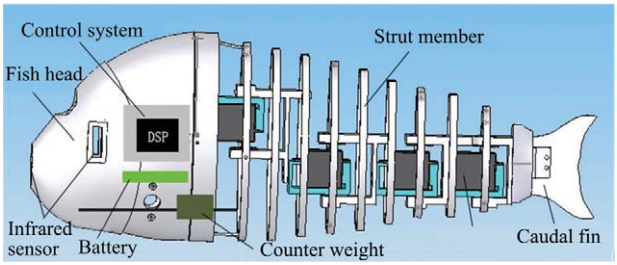

Fig. 1 The mechanical structure of the robotic fish.

2.2 Electronics design of the robotic fish

The robotic fish has capability of swimming in two modes: wireless control and autonomous swimming. When the robotic fish is working in wireless control mode, the movement is manipulated by wireless controller system which is made up of joystick, PC and wireless communication module (Fig. 2). The mode of autonomous swimming is realized based on the infrared sensors equipped on the head module. In the case of no wireless communication and no detection of the infrared sensors, the robotic fish swims autonomously by changing the swimming movements from one to another designed in advance. When the obstacles are detected by the infrared sensors, the robotic fish can round them by taking an appropriate turn with a desired speed.

The movement of the robotic fish and signal processing are operated by the main controller board installed in the head module. The main processor of the main controller board is the microcontroller TMS320 LF2407 (DSP) which offers a mass of application modules such as PLL Clock, JTAG port, CAN, SPI module, Serial Communications Interface (SCI) module, Analog-to-Digital Converter (ADC) module and Event Manager (EV) module *etc.*(Fig. 3). In our work, the SCI module is used to receive the instruction from the controller system and send the state to the actuator as a feedback, and the ADC module is used to process the signal received from the infrared sensors. The EV module generates Pulse Width Modulation (PWM) signals for driving the servomotor.

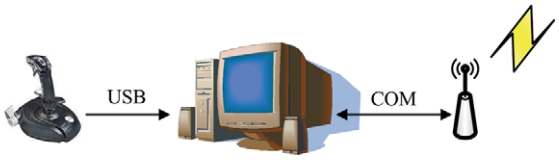

Fig. 2 The transmitter system.

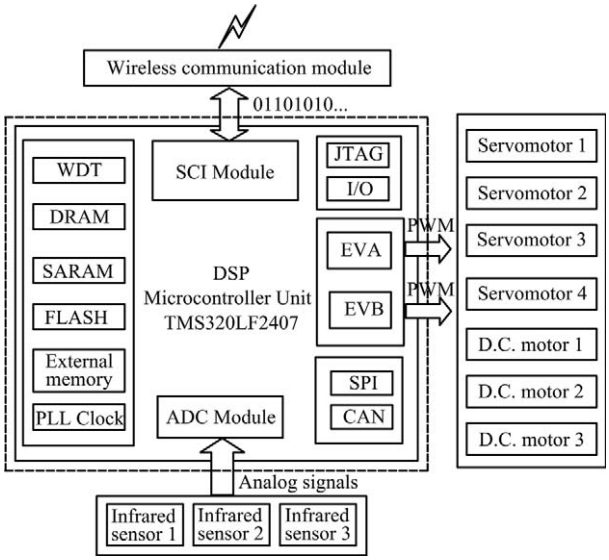

Fig. 3 The function structure of the main processor.

2.3 Locomotion control of robotic fish

The robotic fish is modeled as the *carangiform* fish which swim by swaying the 2/3 posterior part of the body[12–15], and the undulation motion extends from the anterior part to the posterior part. The robotic fish can be considered as a skeleton model (Fig. 4).

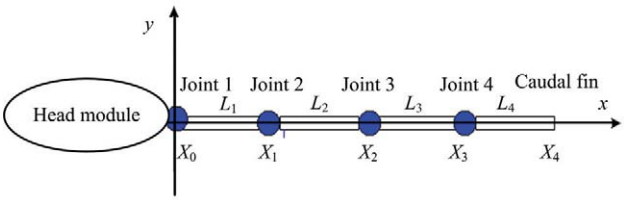

Fig. 4 Simplified model of the robotic fish.

According to Lighthill's work[16], the movement of the robotic fish can express as

$$y_{\text{body}}(x,t) = (C_1 x + C_2 x^2)\sin(kx + \omega t) , \qquad (1)$$

where $y_{\text{body}}(x,t)$ is the transverse displacement of the robotic fish along the x-axis at time t, C_1 and C_2 are the linear coefficient and the quadratic coefficient of the wave amplitude envelope respectively, $k = 2\pi/\lambda$ is the

wave number and λ is the wave length, $\omega = 2\pi f$ is the wave frequency and f is the propelling frequency.

As found in Ref. [17], the caudal fin of fish involves in two motions simultaneously: the heaving and pitching motions. The phases of the two motions are different. Hence, the motion of the robotic fish is divided into two parts: the body undulation and the heaving and pitching motions of the caudal fin. As the processor DSP can only deal with the digital signals, the undulation equation should be discretized. Based on Eq. (1), the movement of the robotic fish is discretized about time t and expressed in body undulation equation and caudal fin oscillation equation, described as

$$y_{\text{body}}(x_i) = (C_1 x_i + C_2 x_i^2)\sin(k x_i - 2\pi \frac{n}{M}) \ , \qquad (2)$$

$$\begin{cases} y_{\text{tail}}(x_4) = y_{\text{body}}(x_3) + L_4 \times \sin\theta \\ \theta = \theta_{\max} \sin(k x_3 - 2\pi \dfrac{n}{M} + \phi) \end{cases} . \qquad (3)$$

In Eq. (2), $i = 0, 1, 2, 3$, x_i denotes the displacement of Joint 1, Joint 2, Joint 3 and Joint 4 along x-axis respectively, and in Eq. (3), $y_{\text{tail}}(x_4)$ is the transverse displacement of the caudal fin along the y-axis, which consists of heaving motion ($y_{\text{body}}(x_3)$) and pitching motion ($L_4 \times \sin\theta$), x_3 is the displacement of Joint 4 (e.g. caudal swing axis) along x-axis, x_4 is the displacement of the end of the caudal fin along x-axis, L_4 is the length of caudal fin, $\theta_{\max}$ is the maximum attack angle[18,19], M is defined as a discrete number that divides a period into small intervals, n counts from 0 to $M-1$, while ϕ represents the phase difference between the heaving and the pitching motions.

The velocity of the robotic fish is influenced by the characteristic parameters mentioned above. First of all, C_1 and C_2 have direct influence on the maximum amplitude, λ plays notable role in undulation classification affecting the velocity and the efficiency of the fish; M has close relationship with the frequency f; ϕ affects the force generated by the caudal fin, which may be thrust or resistance determined by the value of ϕ. The influences of these parameters are investigated in the experiments. The specification of the robotic fish used for the experiment is listed in Table 1, and the robotic fish in swimming is shown in Fig. 5.

Table 1 Specification of the robotic fish

Robot fish	Specifications
Dimension	605 mm × 80 mm × 200 mm
Weight	3.8 kg
Degree of freedom	4
Microcontroller	TMS320LF2407
Actuator	Servomotor
Power source	6V Ni-H battery, 2500 mAh
Sensors	Infrared sensors
Control mode	(1) Radio control (2) Autonomous swim

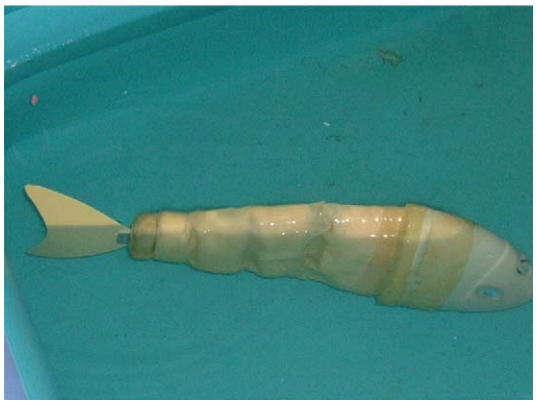

Fig. 5 The robotic fish in swimming.

3 Experiments

To investigate the factors influencing the forward velocity, first we investigate how the forward velocity is affected by several main parameters including the frequency f, the amplitude A, the wave length λ, the phase difference ϕ and the coefficient C_1.

The experiments were conducted in a non-cover tank (4 m × 2 m × 1 m). To collect more detailed and accurate information of the experiments, a high-speed digital vidicon was adopted to record the instantaneous movement of the robotic fish, as shown in Fig. 6. The high-speed digital vidicon is made up of high-speed mega-pixel CMOS camera (Mikrotron MC1310), digital video capture card (IO industries CLFC) and high-speed hard-disk. The highest resolution of collected images is 1280 pixel × 1024 pixel, and the highest acquisition speed is 500 frames·s^{-1}. In our experiments, the acquisition speed is 30 frames·s^{-1}, and the image resolution is 1280 pixel × 1024 pixel. The collected images were imported into a personal computer then were processed using a custom-designed program.

During the experiments, the power of the robotic fish was supplied by a DC Power Supply through two long sealed wires instead of the battery fixed in the robotic fish, under the consideration of the coequal condition of the experiments.

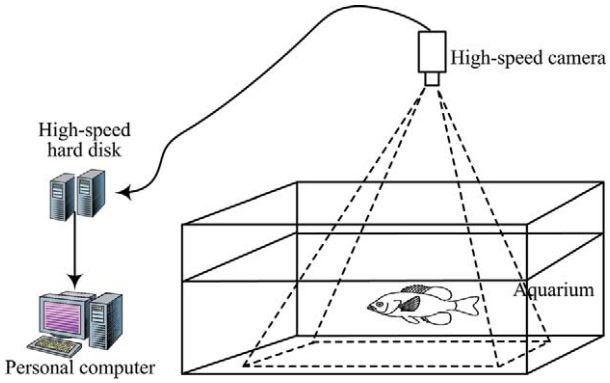

Fig. 6 Experiment instrument set-up.

4 Results and discussion

4.1 Relationship between velocity and swaying frequency

To find out the effect of frequency f on the forward velocity of the robotic fish, we changed the frequency from f_1 to f_7, with the other parameters unchanged. For each frequency, the experiment was conducted for 5 times, then the results were calculated by average and the standard deviation was also given. For detailed comparison, three groups of experiments are conducted by changing the maximum amplitude A. V_{A1}, V_{A2} and V_{A3} are used to denote these three groups of experiments respectively, which are reflected by the three curves of Fig. 7. The results are shown with two vertical axes which denote the velocity and the body length velocity respectively. For simplicity and convenience, we define an experimental parameter matrix as

$$\begin{bmatrix} V_{A1} \\ V_{A2} \\ V_{A3} \end{bmatrix} = \begin{bmatrix} f_{i=1,\ldots,7} & A_1 & R & \phi & C_1 \\ f_{i=1,\ldots,7} & A_2 & R & \phi & C_1 \\ f_{i=1,\ldots,7} & A_3 & R & \phi & C_1 \end{bmatrix}, \quad (4)$$

where f_i represents $\{f_1, f_2, \ldots, f_7\}$, R is defined as relative wave length, which is the ratio of the fish's oscillatory length to the wave length.

As shown in Fig. 7, the forward velocity increases with the frequency and arrives peak at the frequency value of 1.67 Hz, then decreases as the frequency increases. The cause is the speed limit of the servomotor. Consequently, the desired amplitude can not be achieved at high frequency. The three curves by varying the maximum amplitude trend are consistent, and all have a maximum velocity at the frequency 1.67 Hz. The maximum velocity of this experiment is 0.28 $m \cdot s^{-1}$, which is equivalent to 0.47 body length per second.

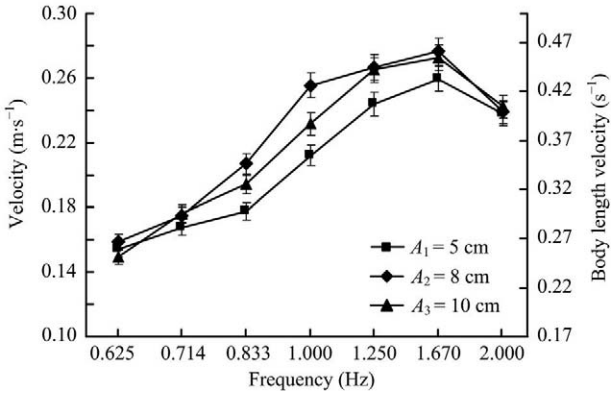

Fig. 7 Forward velocity with different frequencies. $R = 0.5$, $C_1 = 0.08$, $\phi = 90°$, the standard deviations are among the interval (0.0013, 0.0045) $m \cdot s^{-1}$.

4.2 Relationship between velocity and amplitude

The experimental parameter matrix is summarized as

$$\begin{bmatrix} V_{f1} \\ V_{f2} \\ V_{f3} \end{bmatrix} = \begin{bmatrix} f_1 & A_{i=1,\ldots,5} & R & \phi & C_1 \\ f_2 & A_{i=1,\ldots,5} & R & \phi & C_1 \\ f_3 & A_{i=1,\ldots,5} & R & \phi & C_1 \end{bmatrix}, \quad (5)$$

where A_i represents $\{A_1, A_2, \ldots, A_5\}$.

This experiment was conducted to find out how the maximum amplitude affects the velocity by changing the maximum amplitude from 2 cm to 10 cm.

As shown in Fig. 8, the velocities, with the frequencies of 1 Hz and 1.67 Hz, reach their maximum at the amplitude of 6 cm, up to 10 % of the body length. When the frequency is 0.83 Hz, the velocity gets its maximum at the amplitude of 4 cm, mainly because of the lower frequency. The velocity at $A = 10$ cm is smaller then that at $A = 8$ cm. According to the conclusion of Triantafyllou *et al*., for high propulsion efficiency, the amplitude of the *carangiform* fish should not go beyond 10% of the body length[12,17]. In this experiment, the results accord with this conclusion.

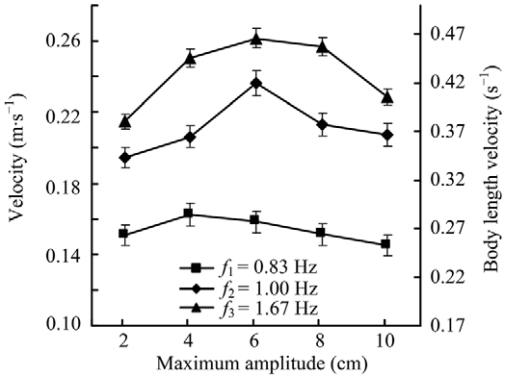

Fig. 8 Forward velocity with different maximum amplitude.

$R = 0.5$, $C_1 = 0.08$, $\phi = 90^\circ$, the standard deviations are among the interval (0.0010, 0.0051) m·s^{-1}.

4.3 Relationship between velocity and wave length

In order to investigate the influence of the wave length on the forward velocity, the parameter R is used to describe wave length instead of λ. Fish can be divided as *ostraciiform*, *thunniform*, *carangiform* and *anguilliform* as the value of R increases. In this experiment, R is set from 0 to 1, the experimental parameter matrix can be expressed as

$$\begin{bmatrix} V_{f1} \\ V_{f2} \\ V_{f3} \end{bmatrix} = \begin{bmatrix} f_1 & A & R_{i=1,\ldots,8} & \phi & C_1 \\ f_2 & A & R_{i=1,\ldots,8} & \phi & C_1 \\ f_3 & A & R_{i=1,\ldots,8} & \phi & C_1 \end{bmatrix}, \quad (6)$$

where R_i represents $\{R_1, R_2, \ldots, R_8\}$.

In Fig.9, the velocity increases linearly with R to its peak, then decreases as R increases continuously. Under the limited performance of the servomotor, the velocity arrives at the maximum 0.35 m·s^{-1} (0.58 body length per second), at the point $R = 0.875$.

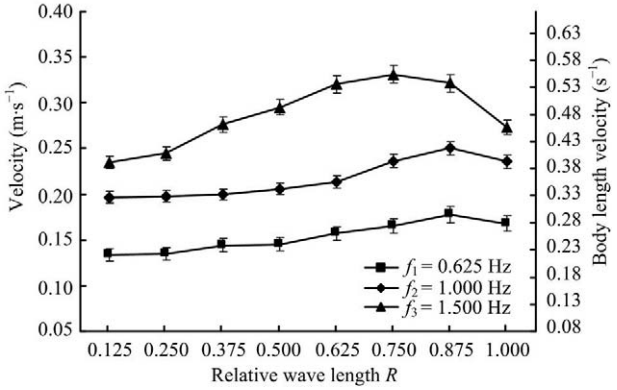

Fig. 9 Forward velocity with relative wave length.

$A = 5$ cm, $C_1 = 0.08$, $\phi = 90^\circ$, the standard deviations are among the interval (0.0011, 0.0043) m·s^{-1}.

4.4 Relationship between velocity and phase difference in heaving and pitching motions

The heaving and pitching motions of the caudal fin do not occur in the same phase, there is a phase difference between them. The research on propulsive efficiency of oscillating foils by Triantafyllou *et al*.[12,17] reveals that the pitching motion should lead the heaving motion by about 75°. So we focus on the effect of the phase difference, and express the experimental parameter matrix as

$$\begin{bmatrix} V_{f1} \\ V_{f2} \\ V_{f3} \end{bmatrix} = \begin{bmatrix} f_1 & A & R & \phi_{i=1,\ldots,10} & C_1 \\ f_2 & A & R & \phi_{i=1,\ldots,10} & C_1 \\ f_3 & A & R & \phi_{i=1,\ldots,10} & C_1 \end{bmatrix}, \quad (7)$$

where ϕ represents $\{\phi_1, \phi_2, \ldots, \phi_{10}\}$.

As shown in Fig. 10, the three curves have the same tendency to reach the maximum velocity at the phase difference of 70°. When the phase difference is 70°, the caudal fin is moving upwards. Because of the resistance of the water, the caudal fin is deformed from the ideal shape to a new curved shape, so the actual phase difference is larger than 70°, reaches to 75° nearly, as shown in Fig. 11.

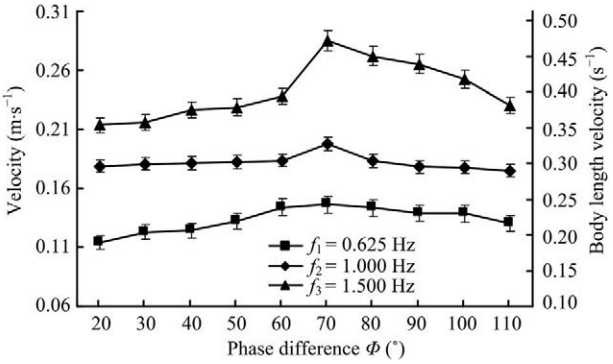

Fig. 10 Forward velocity with phase difference.

$A = 5$ cm, $R = 0.5$, $C_1 = 0.08$, the standard deviations are among the interval (0.0023, 0.0055) m·s^{-1}.

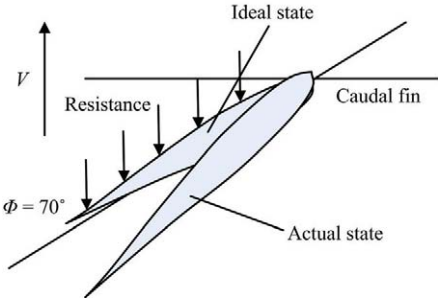

Fig. 11 Sketch depicting the deformation of the caudal fin.

Therefore, when the caudal fin is not a rigid foil but a deformable plate, the phase difference of the heaving and pitching motions should be set lower than 75° for getting higher velocity.

4.5 Relationship between velocity and coefficient C_1

To observe the impact of the coefficient of the wave amplitude envelope on the forward velocity, the linear coefficient C_1 is chose as the considering factor, and the experimental parameter matrix is given by

$$\begin{bmatrix} V_{C11} \\ V_{C12} \\ V_{C13} \end{bmatrix} = \begin{bmatrix} f & A_1 & R & \phi & C_{1i=1,\ldots,5} \\ f & A_2 & R & \phi & C_{1i=1,\ldots,5} \\ f & A_3 & R & \phi & C_{1i=1,\ldots,5} \end{bmatrix}, \quad (8)$$

where C_{1i} represents $\{C_{11}, C_{12},\ldots, C_{15}\}$.

As shown in Fig. 12, when the maximum amplitude is a constant, the envelope of the undulation changes with C_1. When C_1 increases, the envelope will get close to straight line gradually. When C_1 is small, the amplitude of the part near the fish body gravity center is small. As shown in Fig. 13, the three curves have the same tendency that the velocity does not change significantly, and the phase difference decreases when C_1 get higher than 0.1. When C_1 increases, the robotic fish moves as rolling and yawing. It is worth mentioning that the higher C_1 brings stronger movement of the part near the robotic fish body gravity center, and this can lead to an unstable swimming.

5 Conclusions and future work

A *carangiform* robotic fish with 4-DoF tail has been developed which is capable of swimming under two modes of radio control and autonomous swim. The main emphasis of the paper is to investigate experimentally the effects of the characteristic parameters on the robotic fish prototype.

Some conclusions are derived from the experiments:

(1) The cruise velocity of the robotic fish increases with the frequency, and affected by the servomotor performance.

(2) When the maximum amplitude gets to nearly 10% of the body length, the cruise velocity reaches the maximum. This is the same observation made by Triantafyllou[17] in their experiment on oscillating foils.

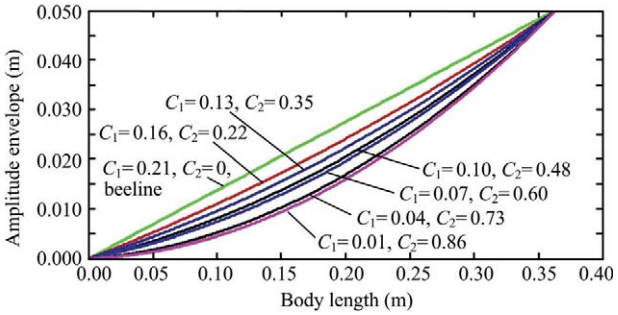

Fig. 12 Inferences of C_1 on the amplitude envelope.

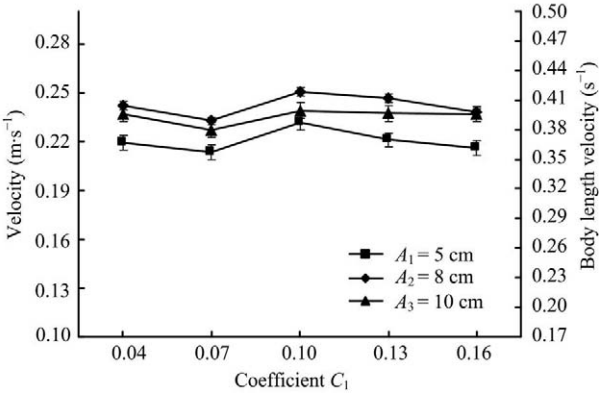

Fig. 13 Forward velocity with different coefficients C_1. R = 0.5, ϕ = 90°, f = 1 Hz, the standard deviations are among the interval (0.0011, 0.0043) m·s^{-1}.

(3) The robotic fish swims at the highest velocity when R is 0.875.

(4) In our experiment, the robotic fish with plastic caudal fin has the peak velocity when the phase difference is fixed at 70°, however, the phase difference should be higher than 70°, if the experiment was conducted on the rigid foil.

(5) The influence of the coefficient C_1 on the velocity is not so obvious, although the velocity will decrease as C_1 increase beyond a certain value.

In future work, more experiments will be conducted to study the swimming efficiency and the maneuverability performance, as well as the performance of ascending and submerging. To collect more detailed and accurate results, more sensors such as pressure sensors, acceleratometer and 3D obliquity detectors will be integrated in the sensing system.

Acknowledgement

The authors thank Prof. K. H. Low sincerely for his helpful comments to the manuscript.

References

[1] Webb P W. Form and function in fish swimming. *Scientific American*, 1984, **25**, 58–68.

[2] Triantafyllou M S, Triantafyllou G S. An efficient swimming machine. *Science American*, 1995, **272**, 64–70.

[3] Mason R, Burdick J W. Experiments in *carangiform* robotic fish locomotion. *Proceedings of International Conference Robotics and Automation*, San Francisco, USA, 2000, 312–317.

[4] Mason R, Burdick J. Construction and modelling of a *carangiform* robotic fish. In: Corke P I, Trevelyan J P (eds), *Experimental Robotics* VI, Springer, London, 1999, 235–242.

[5] Kato N. Control performance in the horizontal plane of a fish robot with mechanical fins. *IEEE Journal of Oceanic Engineering*, 2000, **25**, 121–129.

[6] Liu J D, Dukes I, Hu H S. Novel mechatronics design for a robotic fish. *IEEE*/*RSJ International Conference on Intelligent Robots and Systems*, Edmonton, Canada, 2005, 2077–2082.

[7] Liu J D, Hu H S, A 3D simulator for autonomous robotic fish. *International Journal of Automation and Computing*, 2004, **1**, 42–55.

[8] Liu J D, Hu H S. Mimicry of sharp turning behaviours in a robotic fish. *Proceedings of the IEEE International Conference on Robotics and Automation*, Barcelona, Spain, 2005, 3329–3334.

[9] Low K H, Willy A. Development and initial investigation of NTU robotic fish with modular flexible fins. *IEEE International Conference on Mechatronics and Automation*, Niagara Falls, Canada, 2005, 958–963.

[10] Low K H. Parametric study of modular and reconfigurable robotic fish with oscillating caudal fin mechanisms. *IEEE International Conference on Mechatronics and Automation*, Harbin, China, 2007, 123–128.

[11] Malcolm A M, Fontaine E, Burdick J W. Designing future underwater vehicles: Principles and mechanisms of the weakly electric fish. *IEEE Journal of Oceanic Engineering*, 2004, **29**, 651–659.

[12] Sfakiotakis M, Lane D M, Davies J B C. Review of fish swimming modes for aquatic locomotion. *IEEE Journal of Oceanic Engineering*, 1999, **34**, 237–252.

[13] Yu J Z, Wang L. Parameter optimization of simplified propulsive model for biomimetic robot fish. *IEE*E *International Conference on Robotics and Automation*, Barcelona, Spain, 2005, 3306–3311.

[14] Yu J Z, Wang L. Design framework and motion control for biomimetic robot fish. *IEEE International Symposium on Intelligent Control*, Limassol, Cyprus, 2005, 1435–1440.

[15] Hu Y H, Wang L, Zhao W, Wang Q, Zhang L. Modular design and motion control of reconfigurable robotic fish. *IEEE Conference on Decision and Control*, New Orleans, USA, 2007, 5156–5161.

[16] Lighthill M J. Note on the swimming of slender fish. *Journal of Fluids Mechanics*, 1960, **9**, 305–317.

[17] Triantafyllou G S, Triantafyllou M S, Grosenbauch M. Optimal thrust development in oscillating foils with application to fish propulsion. *Journal of Fluids Structures*, 1993, **7**, 205–224.

[18] Anderson J M, Streitlien K, Barrett D S, Triantafyllou M S. Oscillating foils of high propulsive efficiency. *Journal of Fluids Structures*, 1998, **360**, 41–72.

[19] Guo S X, Okuda Y, Asaka K. A novel type of underwater micro biped robot with multi DOF. *Proceedings of the IEEE International Conference on Robotics and Automation*, New Orleans, USA, 2004, **5**, 4881–4886.